Intramolecular Energy Hopping and Energy Trapping in Polyphenylene Dendrimers with Multiple Peryleneimide Donor Chromophores and a Terryleneimide Acceptor Trap Chromophore

Michael Maus,[†] Rina De,[†] Marc Lor,[†] Tania Weil,[‡] Sivaprasad Mitra,[†] Uwe-M. Wiesler,[†] Andreas Herrmann,[‡] Johan Hofkens,[†] Tom Vosch,[†] Klaus Müllen,[‡] and Frans C. De Schryver*[,†]

Contribution from the Department of Chemistry, Katholieke Universiteit Leuven, Celestijnenlaan 200F, 3001 Heverlee, Belgium and Max-Planck-Institut für Polymerforschung, Ackermannweg 10, 55128 Mainz, Germany

Received March 1, 2001. Revised Manuscript Received May 4, 2001

Abstract: Intramolecular Förster-type excitation energy transfer (FRET) processes in a series of first-generation polyphenylene dendrimers substituted with spatially well-separated peryleneimide chromophores and a terryleneimide energy-trapping chromophore at the rim were investigated by steady-state and time-resolved fluorescence spectroscopy. Energy-hopping processes among the peryleneimide chromophores are revealed by anisotropy decay times of 50−80 ps consistent with a FRET rate constant of $k_{hopp} = 4.6$ ns^{-1}. If a terryleneimide chromophore is present at the rim of the dendrimer together with three peryleneimide chromophores, more than 95% of the energy harvested by the peryleneimide chromophores is transferred and trapped in the terryleneimide. The two decay times ($\tau_1 = 52$ ps and $\tau_2 = 175$ ps) found for the peryleneimide emission band are recovered as rise times at the terryleneimide emission band proving that the energy trapping of peryleneimide excitation energy by the terryleneimide acceptor occurs via two different, efficient pathways. Molecular- modeling-based structures tentatively indicate that the rotation of the terryleneimide acceptor group can lead to a much smaller distance to a single donor chromophore, which could explain the occurrence of two energy-trapping rate constants. All energy-transfer processes are quantitatively describable with Förster energy transfer theory, and the influence of the dipole orientation factor in the Förster equation is discussed.

1. Introduction

Dendrimers have drawn lots of attention because of their highly branched structures capable of being used as building blocks for photonic devices.[1,2] Several reports on dendrimers have been published in different areas such as guest-host chemistry,[3] analytical chemistry,[4] optoelectronics,[5] catalysis,[6] and biology.[7] As dendrimers are also used to mimic the photosynthetic-light-harvesting antenna system, different types of dendritic and related chromophore assemblies have been designed and investigated to harvest light energy.[8−22] A general pursuing sophisticated goal is to combine the artificial antenna system with an efficient energy trap to control the energy pathways. Only a few examples have recently been reported.[8−13] However, the absence of shape persistence usually prevents a fully quantitative description.

Recently, investigations of dendrimers with a polyphenyl core around a central biphenyl unit decorated at the rim with

* Corresponding author. E-mail: frans.deschryver@chem.kuleuven.ac.be.
[†] Katholieke Universiteit Leuven.
[‡] Max-Planck-Institut für Polymerforschung.

(1) Bosman, A. W.; Janssen, H. M.; Meijer, E. W. *Chem. Rev.* **1999**, *99*, 1665.
(2) Aida, T.; Jiang, D.-L. *J. Am. Chem. Soc.* **1998**, *120*, 10985.
(3) Frechet, J. M. *Science* **1994**, *263*, 1710.
(4) Matthews, O. A.; Shipway, A. N.; Stoddart, J. F. *Prog. Polym. Sci.* **1998**, *23*, 1.
(5) Atwood, J. L.; Davies, J. E. C.; Macnicol, D. D.; Vögtle, F.; Lehn, J.-M. *Comprehensive Supramolecular Chemistry*; Pergamon Press: Oxford, 1996.
(6) Stinson, S. C. *Chem. Eng. News* **1997**, *75*, 28.
(7) Haensler, J.; Szoka, F. C., Jr. *Bioconjuate Chem.* **1993**, *4*, 372.
(8) Adronov, A.; Gilat, S. L.; Frechet, J. M. J.; Ohta, K.; Neuwahl, F. V. R.; Fleming, G. R. *J. Am. Chem. Soc.* **2000**, *122*, 1175.
(9) Devadoss, C.; Bharati, P.; Moore, J. S. *J. Am. Chem. Soc.* **1996**, *118*, 9635.
(10) Schenning, A. P. H. J.; Peeters, E.; Meijer, E. W. *J. Am. Chem. Soc.* **2000**, *122*, 4489.
(11) Li, Feirong; Yang, S. I.; Ciringh, Y.; Seth, J.; Martin, C. H.; Singh, D. L.; Kim, D.; Birge, R. R.; Bocian, D. F.; Holten, D.; Lindsey, J. S. *J. Am. Chem. Soc.* **1998**, *120*, 10001−10017.
(12) Brodard, P.; Matzinger, S.; Vauthey, E.; Mongin, O.; Papamicaël, C.; Gossauer, A. *J. Phys. Chem. A* **1999**, *103*, 5858.
(13) Jullien, L.; Canceill, J.; Valeur, B.; Bardez, E.; Lefevre, J. P.; Lehn, J. M.; MarchiArtzner, V.; Pansu, R. *J. Am. Chem. Soc.* **1996**, *118*, 5432.
(14) Hofkens, J.; Latterini, L.; De Belder, G.; Gensch, T.; Maus, M.; Vosch, T.; Karni, Y.; Schweitzer, G.; De Schryver, F. C.; Herrmann, A.; Müllen, K. *Chem. Phys. Lett.* **1999**, *304*, 1.
(15) Karni, Y.; Jordens, S.; De Belder, G.; Hofkens, J.; Schweitzer, G.; De Schryver, F. C.; Herrmann, A.; Müllen, K. *J. Phys. Chem. B* **1999**, *103*, 9378.
(16) Hofkens, J.; Maus, M.; Gensch, T.; Vosch, T.; Cotlet, M.; Köhn, F.; Herrmann, A.; Müllen, K.; De Schryver, F. C. *J. Am. Chem. Soc.* **2000**, 122, 9728.
(17) Zhang, H.; Grim, P. C. M.; Foubert, P.; Vosch, T.; Vanoppen, P.; Wiesler, U.-M.; Berresheim, A. J.; Müllen, K.; De Schryver, F. C. *Langmuir* **2000**.
(18) Weil, T.; Wiesler, U.-M.; Herrmann, A.; Bauer, R.; Hofkens, J.; De Schryver, F. C.; Müllen, K., submitted.
(19) Maus, M.; Mitra, S.; Lor, M.; Hofkens, J.; Weil, T.; Herrmann, A.; Müllen, K.; De Schryver, F. C. *J. Phys. Chem. A* **2001**, *105*, 3961.
(20) Yeow, E. K. L.; Ghiggino, K. P.; Reek, J. N. H.; Crossley, M. J.; Bosman, A. W.; Schenning, A. P. H. J.; Meijer, E. W. *J. Phys. Chem. B* **2000**, *104*, 2596.
(21) Berberan-Santos, M. N.; Canceill, J.; Gratton, E.; Jullien, L.; Lehn, J.-M.; So, P.; Sutin, J.; Valeur, B. *J. Phys. Chem.* **1996**, *100*, 15.
(22) Berberan-Santos, M. N.; Choppinet, P.; Fedorov, A.; Jullien, L.; Valeur, B. *J. Phys. Chem.* **1999**, *121*, 2526.

10.1021/ja010570e CCC: $20.00
Published on Web 06/20/2001

Chart 1. Molecular Structure of the (a) Dendrimers and (b) Chromophores **PI** and **TI** (in **TI** is R, a Vinyl Group for the Model Compound **TI-m** and a Part of the Aromatic Dendrimer Arm in the Dendrimer); (c) An Example of the Three-Dimensional Structure of **G1R3_p** and (d) **G1R3Ter_p**

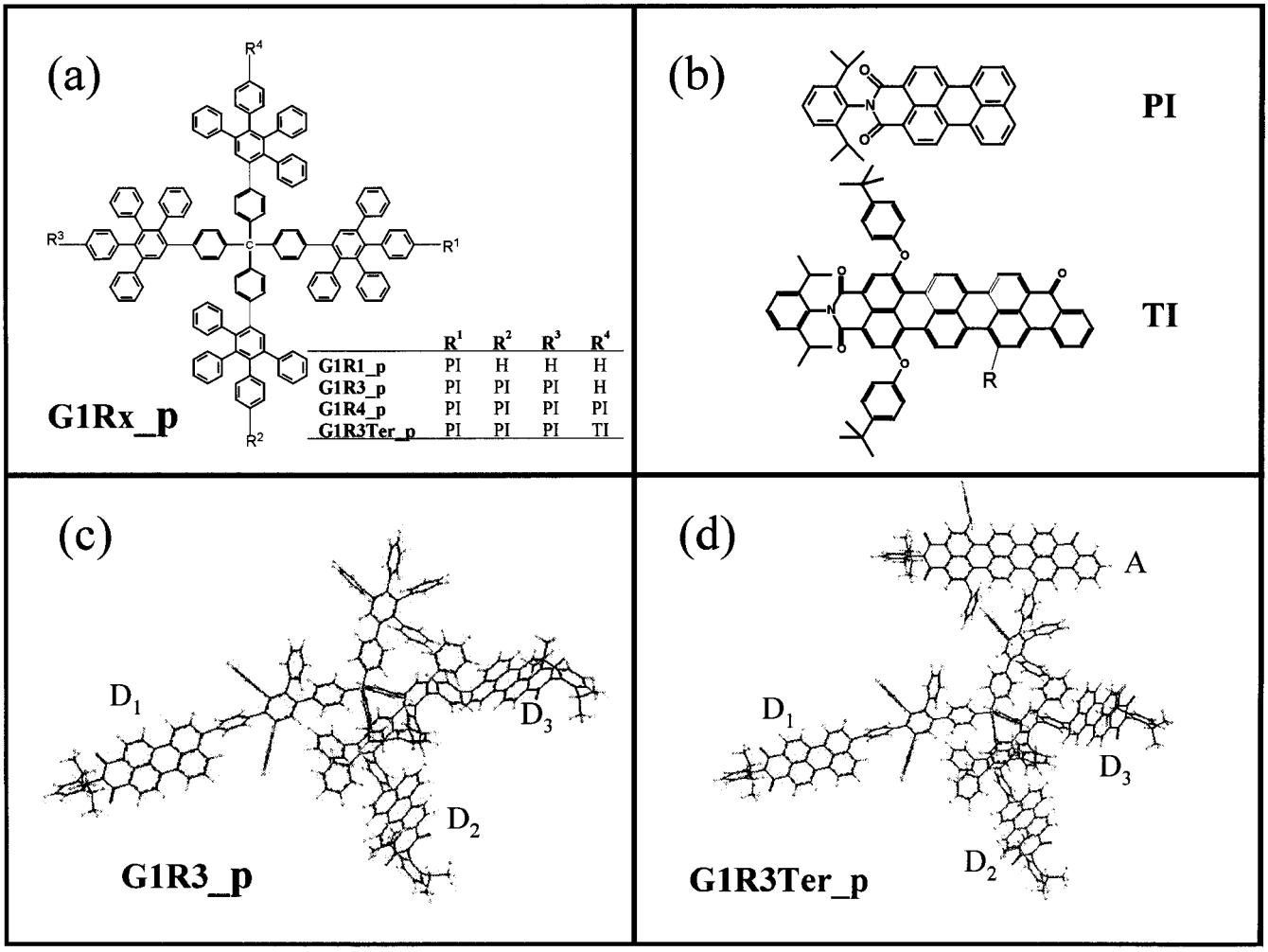

peryleneimide chromophores have been reported[14−17] at the ensemble and single molecule level leading to the understanding of the time and space resolved excited-state behavior of these peryleneimide dendrimers. It has been shown that the conformational distribution plays an important role in the dynamics of the photophysical processes involved.

With the aim of getting a better control over the spatial and orientational distribution of the peripheral chromophores, a series of dendrimers with a stiff core has been prepared[18] consisting of a central sp^3 hybridized carbon to which the chromophores are arranged along the corners of the tetrahedron.

In a first series of systems, the chromophores are linked at the meta position of the outer phenyl group.[19] In these dendrimers, a variable number (1−4) of peryleneimides are placed at the end of the polyphenyl arms. Direct excitation of the peryleneimide chromophore results in energy hopping among identical chromophores. The extent and rate constant of energy hopping was determined. As meta substitution results in a small configurational and conformational fraction of molecules in which peryleneimide leads to an "excited dimer", a series of similar compounds, but with substitution in the para position of the outer phenyl group, was synthesized[18] and is studied here (see Chart 1). Furthermore, to analyze energy transfer to a fluorescent trap, a dendritic structure with three peryleneimides and one teryleneimide is additionally investigated (Chart 1). The ensemble photophysics in toluene of this series of molecules is reported here.

2. Experimental Section

Materials. The synthesis of these rigid dendrimers having a tetrahedral core with a different number of peryleneimide and teryleneimide chromophores on the polyphenylene rim **I** required a novel approach, which is being published separately.[18]

The samples were dissolved in toluene (Aldrich) to have an optical density below 0.1 in a 1 cm cell at the absorption maximum (495 nm), which corresponds to a concentration of $\sim 10^{-7}$ M.

Steady-State Measurements. Steady-state absorption and corrected fluorescence spectra were recorded with Lambda 40 (Perkin-Elmer) and SPEX spectrophotometers, respectively. The fluorescence quantum yields have been determined using a polyphenylene dendrimer (**G1R1_m**) as a reference,[19] that is substituted by a single peryleneimide in meta position.

Picosecond Time-Resolved Measurements. The fluorescence decay times have been determined by the single photon timing method using a setup described previously.[23] In brief, the second harmonic of a Ti: sapphire laser (Tsunami, Spectra Physics) has been used to excite the samples at 488 nm with a repetition rate of 4.09 MHz. The detection system consists of a subtractive double monochromator (9030DS, Sciencetech) and a microchannel plate photomultiplier (R3809U,

(23) Maus, M.; Rousseau, E.; Cotlet, M.; Schweitzer, G.; Hofkens, J.; Van der Auweraer, M.; De Schryver, F. C.; Krueger, A. *Rev. Sci. Instrum.* **2000**, *72*, 36.

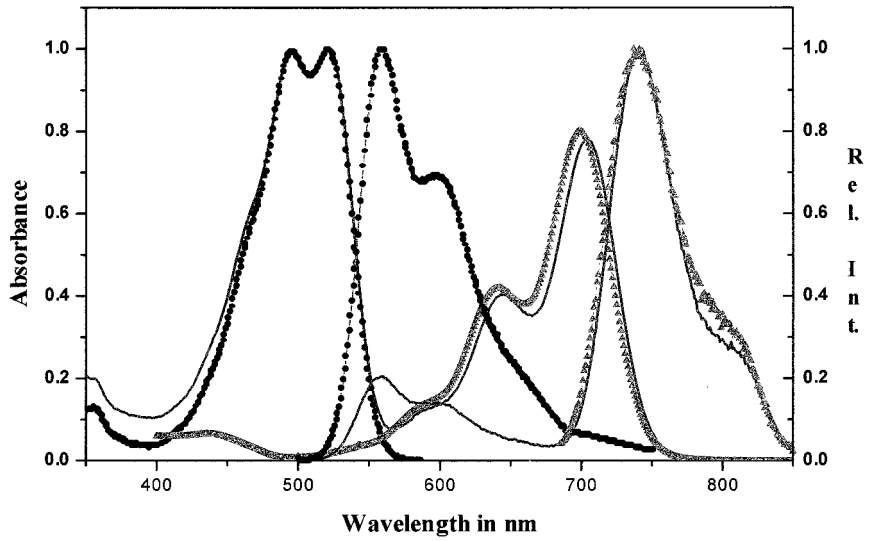

Figure 1. Steady-state absorption and emission spectra of the compounds **G1Rn_p** (circles), the donor acceptor system **G1R3ter_p** (solid lines), and teryleneimide model compound **TI-m**. (triangles).

Hamamatsu). A time-correlated single photon counting PC module (SPC 630, Picoquant GmbH), which has the two constant fraction discriminators (CFD), a time-to-amplitude converter (TAC), and an analog-to-digital converter (ADC) on board, was used to obtain the fluorescence decay histograms in 4096 channels with time increments of 5 or 10 ps. The fluorescence decays have been recorded at three different orientations of the emission polarizer relative to the polarization plane of the excitation light, that is, 54.7° (magic angle), 0° (I_{par}), and 90° (I_{perp}). The magic angle decays were analyzed globally with a time-resolved fluorescence analysis (TRFA) software.[24] The quality of the fits has been judged by the fitting parameters such as χ^2 (<1.2), $Z\chi^2$ (<3) and the Durbin−Watson parameter (1.8 < DW < 2.2) as well as by the visual inspection of the residuals and autocorrelation function.[25] The anisotropy decay as calculated from eq 1

$$r(t) = \frac{I_{par}(t) - I_{perp}(t)}{I_{par}(t) + 2I_{perp}(t)} \tag{1}$$

was fitted by a linear combination of exponentially decaying functions using the Levenberg−Marquard χ^2 minimization on the basis of eq 2

$$\chi^2 = \frac{\sum_{i=1}^{N}[y_i - f(x_i)]^2}{N - P} \tag{2}$$

where N is the number of data points and P is the number of free parameters in the fit function. The anisotropy decay analysis was performed with our global fluorescence decay analysis program TRFA,[24] which takes pulse deconvolution into account.

3. Theoretical Kinetic Model

The theoretical model for the energy hopping among the identical chromophores of **G1R1_p, G1R3_p,** and **G1R4_p** has followed the same method as described in ref 19 using uniform rate constants for the energy hopping (k_{hopp}) and a uniform rotational relaxation (Θ_{rot}) and fluorescence lifetime (τ_f). The fluorescence intensity decay $I_f(t)$ is then described by a single-exponential function with an arbitrary amplitude α according to eq 3,

$$I_f(t) = \sum_{1}^{i} \frac{\alpha}{i} P_i(t) = \alpha\, e^{-t/\tau f} \tag{3}$$

and the anisotropy decay is expressed by eq 4.[19]

$$r(t) = r_1(t) = \frac{r_0}{i}[e^{-t/(\theta_{rot})} + (i-1)e^{-(ik_{hopp} + \theta_{rot}^{-1})t}] \tag{4}$$

This simple model predicts a double-exponential anisotropy decay with an amplitude ratio of $(i - 1)$. If rotational movements are absent ($\Theta_{rot}^{-1} = 0$), a constant term r_0/i gives the well-known leveling off at long times.[12,20−22,26]

In case of the presence of an energy trap, the function for the anisotropy decay remains the same as far as the fluorescence of the donor chromophores is concerned. However, to obtain an analytical expression for the intensity decay of a molecular system consisting of i donor chromophores and an emitting-energy trap A, the following master equation has to be solved

$$\frac{d\boldsymbol{P}}{dt} = \mathbf{K}\mathbf{P} \tag{5}$$

where **P** is the vector of the time-dependent individual excitation probabilities for i donors and a single acceptor

$$\mathbf{P}(t) = \begin{pmatrix} D_1(t) \\ D_2(t) \\ \cdots \\ D_i(t) \\ A(t) \end{pmatrix} \tag{6}$$

and **K** is the matrix of rate constants

(24) Homemade program developed in a cooperation between The Management of Technology Institute (Belarusian State University) and The Division of Photochemistry and Spectroscopy (Katholieke University of Leuven).

(25) (a) O'Connor, D. V.; Phillips, D. *Time-Correlated Single Photon counting*; Academic Press: London, 1984; p 252. (b) Gierer, A.; Wirtz, K. *Z. Naturforsch., A: Phys. Sci.* **1953**, *8*, 532.

(26) *Resonance Energy Transfer*; Andrews, D. L., Demidov, A. D., Eds.; John Wiley & Sons: Chichester, England, 1999.

$$\mathbf{K} = \begin{vmatrix} -\sum_{j=1;j\neq 1}^{i} k_{1j} - k_{1A} - \tau_f(D_1)^{-1} & k_{21} & \cdots & k_{i1} & 0 \\ k_{12} & -\sum_{j=1;j\neq 2}^{i} k_{1j} - k_{2A} - \tau_f(D_2)^{-1} & \cdots & k_{i2} & 0 \\ \cdots & \cdots & \cdots & \cdots & \cdots \\ k_{1i} & k_{2i} & \cdots & -\sum_{j=1;j\neq i}^{i} k_{1j} - k_{iA} - \tau_f(D_i)^{-1} & 0 \\ k_{1A} & k_{2A} & \cdots & k_{iA} & -\tau_f(A)^{-1} \end{vmatrix} \quad (7)$$

where k_{ij} represents the energy-hopping rate constants from donor i to donor j, k_{jA} corresponds to the rate constant for energy trapping of donor j to the acceptor, $\tau_f(D_j)$ and $\tau_f(A)$ are the fluorescence lifetimes of the jth donor and the acceptor chromophore, respectively. For the simplest case of identically and equivalently behaving donor chromophores resulting in full energy-hopping cross talk ($k_{ij} = k_{hopp}$) and a single energy-trapping rate constant ($k_{ja} = k_{trap}$), the intensity decays of the donor and acceptor fluorescence can be described by

$$I_f^D(t) = \alpha \sum_1^i \frac{1}{i} D_i(t) = \alpha\, e^{-(k_{trap}+1/\tau_f)t} \quad (8)$$

$$I_f^A(t) = \gamma A(t) = \frac{\gamma}{k_{trap} + ik_{hopp} + \tau_f(D)^{-1} - \tau_f(A)^{-1}} \times (e^{-t/\tau_f(A)} - e^{-(k_{trap}+1/\tau_f(D))t}) \quad (9)$$

More complex solutions are discussed in the text.

4. Results

Steady-State Spectra. The steady-state absorption and fluorescence spectra of the dendrimers (**G1R1_p, G1R3_p, G1R4_p**) (Figure 1) containing only peryleneimide chromophores are identical, whereas for the dendrimer **G1R3ter_p** (Figure 1) the spectra show the sum of that of peryleneimide and teryleneimide chromophores. The absorption spectra of all the dendritic compounds in toluene show two vibronic maxima at 495 and 520 nm; in addition, the dendrimer **G1R3ter_p** shows three more vibronic bands at 592, 645, and 700 nm due to the teryleneimide chromophore. The fluorescence spectra show emission maxima at 560 and 595 nm for all above-mentioned dendrimers with an additional emission maximum at 730 nm for the dendrimer **G1R3ter_p**. The band at 730 nm is found if the molecule is excited at 680 nm in the teryleneimide absorption band and also at 495 nm in the peryleneimide absorption band. The fluorescence quantum yields ($\phi_f = 0.98 \pm 0.05$) of the dendrimers **G1R1_p, G1R3_p, G1R4_p** have been found to be the same within the experimental error. The intensity of the perylene emission of **G1R3ter_p** has been found to be reduced by 95% based on fluorescence decay measurements (vide infra)

Time-Resolved Measurements. To investigate the excited-state deactivation taking place in these molecules, the time-resolved fluorescence measurements were undertaken. The fluorescence decay times for all the dendrimers were measured in toluene by the single photon counting method, detecting the emission under magic angle condition. The dendrimers were excited at 488 nm, the fluorescence decays were monitored at different emission wavelengths, and the decay traces were globally analyzed. The quality of the fitted decays was judged by the distribution of weighted residuals (R_I) and autocorrelation function (ac). A fluorescence decay trace of **G1R3ter_p** is given in Figure 2 and the respective decay parameters are collected in Table 1.

The global analysis of nine wavelength-dependent fluorescence decays in the range of 550−780 nm results in very good statistical fit quality parameters ($\chi^2 = 1.05$, DW = 1.9, $Z\chi^2 = 1.8$) if two decay times ($\tau_1 = 52$ ps and $\tau_2 = 175$ ps) for the perylene emission band and the same time constants $\tau_1$and τ_2 as two rise times together with the fluorescence lifetime ($\tau_3 = 2.5$ ns) of terryleneimide for the terryleneimide emission band are used. Neglecting of one rise (decay) time leads to a mean rise (decay) time of 148 ps with poor statistical fit quality parameters ($\chi^2 = 2.04$, DW = 1.0, $Z\chi^2 = 39$) proving the necessity of the two decay and rise times τ_1 and τ_2.

In addition, the time-resolved emission spectra were recorded for different time windows (Figure 3). The time zero corresponds to the onset of the first fluorescence photons.

Time-Resolved Polarization Measurements. To get a better insight into the dynamics involved, time-resolved anisotropy measurements were carried out. The anisotropy decay times (Θ) and the associated anisotropy (β) have been determined for all the compounds using eq 10

$$r(t) = \sum \beta_i \exp\left(-\frac{t}{\Theta_i}\right) \quad \text{and} \quad r_0 = \sum_i \beta_i \quad (10)$$

For the dendrimer with one chromophore (**G1R1_p**), a monoexponential function is found to be sufficient to fit the anisotropy decay trace which can be related to the relaxation time of $\Theta_1 = 1.4$ ns ± 30 ps with $\beta_1 = r_0 = 0.34 \pm 0.04$ (Table 2). However, the anisotropy decay traces for the dendrimers having more than one chromophore (**G1R3_p, G1R4_p, G1R3ter_p**) can only be fitted with two exponential decay functions (Figure 4). The magnitude of the long depolarization time component increases as the number of chromophores increases from 1 to 4, while the value of the fast component (Θ_2) changes from 70 ps for **G1R3_p** to 50 ps in **G1R4_p** (Table 2).

5. Discussion

Fluorescence from Localized Species. The steady-state properties of the dendrimers (**G1R1_p, G1R3_p, G1R4_p**) in terms of spectral shape, fluorescence maxima, and fluorescence quantum yield are within experimental error. This differs from observations made for the meta-substituted peryleneimide dendrimers[19] where these steady-state spectral properties are found to be influenced by the formation of an excimer-like species.

Table 1 shows that the lifetimes of **G1R1_p, G1R3_p, G1R4_p** are the same, which is expected as the fluorescence is emitted from peryleneimide chromophores. No long decay component of 7.4 ns is observed as obtained for dendritic structures with a similar core, where the peryleneimide chro-

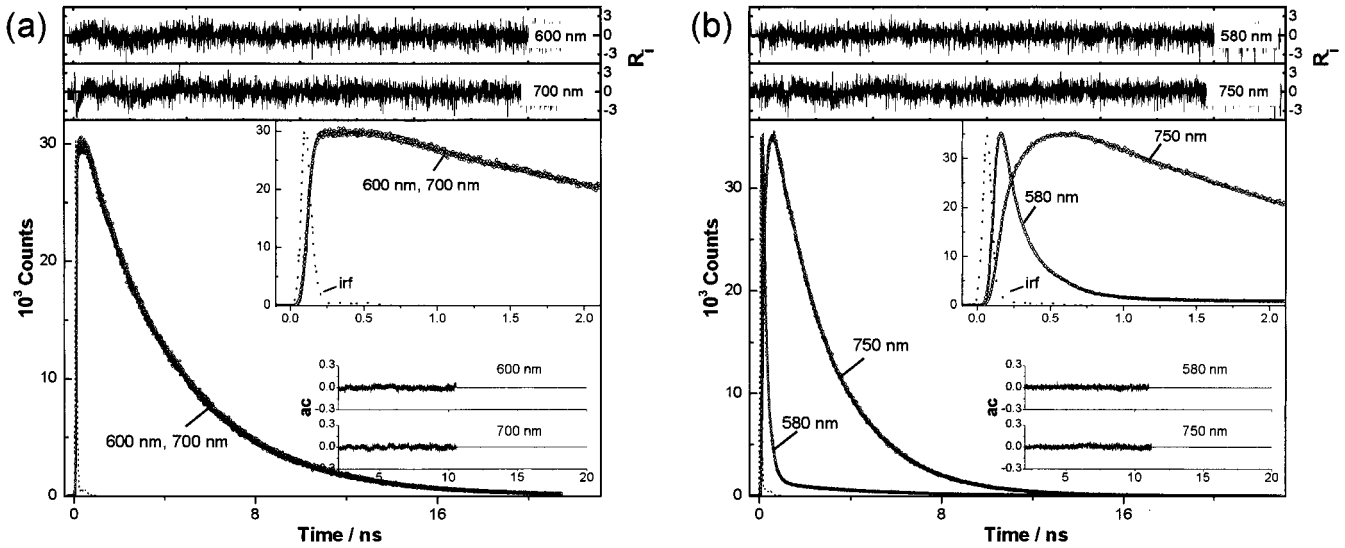

Figure 2. Time-resolved fluorescence decays of (a) **G1R3_p** and (b) **G1R3ter_p** with fits. The upper level shows the weighted distribution of residuals (R_I), and the lower one represents the auto-correlation (ac) functions for the decay. The excitation wavelength, λ_{exc}, is 488 nm.

Table 1. Fluorescence Decay Times (τ_i) and Associated Relative Amplitudes (α_i) for the Dendrimers Measured in Toluene at Room Temperature Using $\lambda_{exc} = 488$ nm

				$\lambda_{flu} = 600$ nm			$\lambda_{flu} = 750$ nm		
compound	τ_1 (ns)	τ_2 (ns)	τ_3 (ns)	α_1 (%)	α_2 (%)	α_3 (%)	α_1 (%)	α_2 (%)	α_3 (%)
G1R1_p	4.0			100					
G1R3_p	4.0			100					
G1R4_p	4.0			100					
G1R3ter_p[a]	0.052	0.175	2.51	62.1	37.9	0	−30.9	−15.7	53.4

[a] 2% of the decay at 600 nm was due to less than 0.1% peryleneimide dendrimer impurity in the sample that could not be separated by purification. This contribution is not considered.

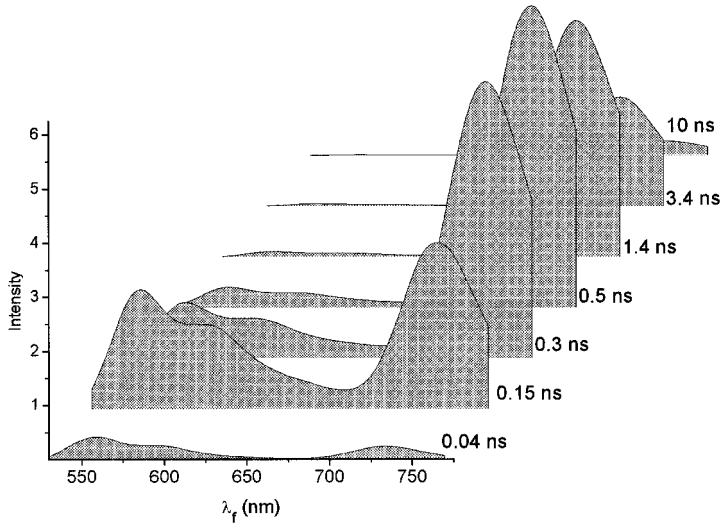

Figure 3. Time-resolved emission spectra of **G1R3ter_p** in toluene. The time zero is defined as the time of the arrival of the first fluorescence photon in the corresponding fluorescence decay. The spectra correspond to the time ranges 0.04 ± 0.04 ns, 0.145 ± 0.065 ns, 0.30 ± 0.095 ns, 0.55 ± 0.15 ns, 1.35 ± 0.65 ns, 3.40 ± 1.40 ns, 9.7 ± 5 ns. They are corrected for the detector−spectral response and the measured time window. The excitation wavelength, λ_{exc}, is 488 nm.

mophores are substituted in the meta position of the pentaphenylbenzene building block[19] instead of the para position for the dendrimers studied here. Therefore, the absence of the long decay component is due to the different position of substitution leading to a better spatial separation of the individual chromophores. This is also supported by a comparison of the molecular mechanics structures of the para- (Chart 1) and meta-substituted dendrimers, since the center-to-center distance among the chromophores is 29 Å for the para series, but only 26 Å for the meta series.

Excitation of the dendrimer **G1R3ter_p** at 495 nm (the peryleneimide absorption maximum) results not only in residual peryleneimide emission but also in emission at 730 nm that corresponds to the teryleneimide emission, which demonstrates unidirectional energy transfer from peryleneimide to the trap teryleneimide chromophore. This energy-trapping process is discussed in detail below. As concerns the localized peryleneimide and terryleneimide fluorescence, both time-resolved and steady-state results indicate the absence of intramolecular excimer-like chromophore interaction also in **G1R3ter_p**.

Table 2. Fitting Parameters of the Fluorescence Anisotropy Decays Measured for the Dendrimers in Toluene with $\lambda_{exc} = 488$ and $\lambda_{flu} = 600$ nm and Calculated Average Peryleneimide−Peryleneimide Distances (d_{FRET})

compound	r_0	Θ_1 (ns)	Θ_2 (ns)	β_1	β_2	β_2/r_0 (%)	d_{FRET} (Å)[a]
G1R1_p	0.34	1.4		0.34			
G1R3_p	0.31	1.6	0.07	0.09	0.22	71	27.3
G1R4_p	0.34	2.0	0.05	0.07	0.27	79	27.4
G1R3ter_p	0.33	2.3	0.075	0.09	0.24	72	27.5

[a] Using $r_0 = 44.3$ Å in eq 16.

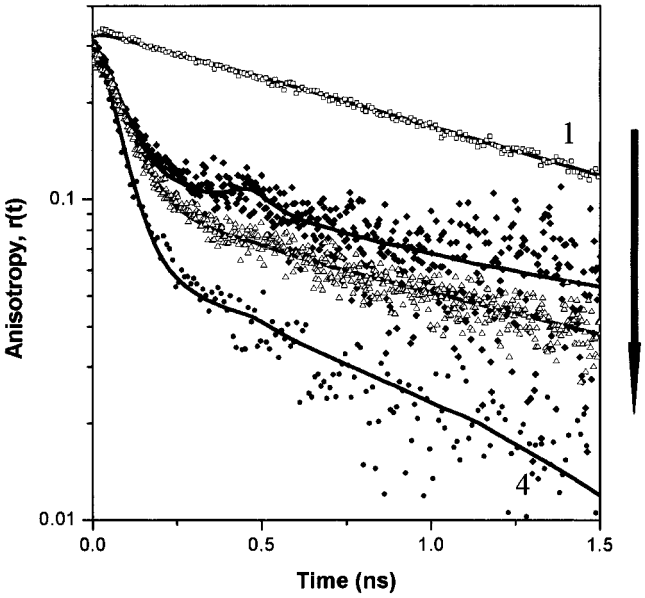

Figure 4. Time-resolved anisotropy decays (scattered symbol) and the fits (solid line) for the dendrimers from 1 to 4: 1, open squares, **G1R1_p**; 2, full diamonds, **G1R3_p**; 3, open triangles, **G1R4_p**; 4, full circles, **G1R3ter_p**. The excitation and emission wavelengths are 488 and 600 nm, respectively.

Size of the Dendrimers. The single anisotropy decay time (Θ_1) of about 1.4 ns (Table 2) for the dendrimer **G1R1_p** obtained from fluorescence anisotropy measurements can be associated with the rotational relaxation time (Θ_{rot}) of the whole dendrimer. The corresponding long polarization time constant (Θ_1) increases to 2.3 ns in **G1R3ter_p**. Assuming a spherical volume of the rotor, the diameters (d_{rot}) can be calculated with eq 11

$$d_{rot} = \sqrt[3]{\frac{6V}{\pi}} \tag{11}$$

on the basis of the Debye−Stokes−Einstein relation given by eq 12

$$\Theta_{rot} = \frac{V\eta fC}{k_B T} \tag{12}$$

where Θ_{rot} is the rotational relaxation time obtained from Θ_1 according to eq 4 and 10 with $k_{hopp} = 4.6$ ns^{-1} (vide infra), V is the hydrodynamic volume, η is the solvent viscosity, k_B is the Boltzmann constant, T is the temperature, f is a form factor set to 1 for spherical objects, and C is a correction factor varying between 0 and 1 depending on sticking or slipping conditions.[25a] On the basis of the Gierer−Wirtz model,[25b] using the calculated van der Waals volumes of solvent and solutes, a correction factor of 0.45 is obtained leading to a hydronamic radius in the order of 25 Å. The resulting increase in *rotational correlation times* for **G1R1_p** to **G1R3ter_p** scales well with the expected increase of the hydrodynamic volume with the introduction of more chromophores in the dendritic structure. Moreover, these values are consistent with the increase of the dimensions deduced from molecular-modeling structures (Chart 1c and 1d)[27] and, as expected, in comparison to the corresponding meta-substituted dendrimers, the rotor diameters are larger in para-substituted dendrimers.

Intramolecular Excitation Energy Hopping. The process of energy hopping can be investigated by time-resolved anisotropy data. The relatively large value for the limiting anisotropy (r_0) of **G1R1_p** confirms an almost parallel orientation of the absorption and emission transition dipole moment for a single chromophore.

In contrast to the mono-exponential anisotropy trace of monochromophoric **G1R1_p**, the corresponding traces of the polychromophoric dendrimers **G1R3_p, G1R4_p, and G1R3ter_p** reveal a second and fast anisotropy decay component in the order of 50−80 ps. This fast depolarization process can be related to excitation energy hopping among the identical peryleneimide chromophores. From the time scale of these processes, it is apparent that the energy hopping takes place through the Förster mechanism in the same way as has been discussed previously for the corresponding meta series of dendrimers.[19] Within the framework of the Förster formulation,[26,28−30] an effective interaction radius (R_0) can be calculated from the steady-state spectra and the fluorescence quantum yield of the donor chromophore (ϕ_D) with the equations (13) and (14)

$$R_0^{\,6} = 8.875 \times 10^{-5} \frac{\kappa^2 \phi_D J}{n^4} \tag{13}$$

where κ^2 is used as a first approximation equal to two-thirds for the usually assumed random orientation of the chromophores, ϕ_D is the donor fluorescence quantum yield, n is the refractive index of the solvent (1.496 for toluene), and J is the spectral overlap integral defined by

$$J = \frac{\int F_D(\lambda)\epsilon_A(\lambda)\lambda^4 \, d\lambda}{\int F_D(\lambda) \, d\lambda} \tag{14}$$

where $\epsilon_A(\lambda)$ represents the molar extinction coefficient of the acceptor, and $F_D(\lambda)$ represents the donor fluorescence spectrum on a wavelength (λ) scale. The calculated values of $R_0 = 38$ Å and $J = 2.5 \times 10^{14}$ M^{-1} cm^{-1} nm^4, using the spectral data ($\epsilon_{max}/3 = 38.300$ M^{-1} cm^{-1},[18] $\phi_f = 98\%$) of the trichromophoric **G1R3_p** compound, are on the typical order of magnitude to be expected for FRET.[31]

Information about the rate constant of hopping (k_{hopp}) through FRET can be derived from the fast anisotropy decay time (Θ_2). However, to take into account the possibility of multiple hopping channels in the case of a multichromophoric system containing identical chromophores among which efficient dipole−dipole interaction occurs, the measured decay time Θ_2 can be related to k_{hopp} according to the energy-hopping model[19] by combining

(27) Spartan Program, Wave function, Inc., 17401 Von Karman Ave., Ste. 370, CA 92612.
(28) Förster, T. *Ann. Phys.* **1948**, *2*, 55.
(29) Duus, J. Ø.; Meldal, M.; Winkler, J. R. *J. Phys. Chem. B* **1998**, *102*, 6413.
(30) Cheung, H. C. In *Topics in Fluorescence Spectroscopy*; Lakowicz, J. R., Ed.; Plenum Press: New York, 1991; Vol. 2, p 127.
(31) A collection of various references can be found in: Haughland, R. P. *Handbook of Fluorescent Probes and Research Chemicals*, 6th ed.; Molecular Probes Inc.: Eugene, OR, 1996; p 46.

$\Theta_{rot} = \Theta_1$, eq 4 and eq 10, giving eq 15

$$k_{hopp} = \frac{1}{i\Theta_2} - \frac{1}{i\Theta_1} \quad (15)$$

where the value of i represents the number of chromophores fully interacting in both forward and backward directions. On the basis of eq 15, a value of around 4.6 ns^{-1} is obtained for k_{hopp} of **G1R3_p**, **G1R4_p**, and **G1R3ter_p**, respectively. It seems surprising that this value is more than twice as large than that ($k_{hopp} = 2$ ns^{-1}) obtained for the meta-substituted dendrimers, even though the interchromophoric distances is ca. 2 Å larger in the para series. In fact, by employing the excited-state lifetime $\tau_D = 4$ ns, using the above derived values of $R_0 = 38$ Å and $k_{FRET} = k_{hopp}$, the calculation of the distance between two chromophores through the Förster eq 16[28]

$$d^6_{FRET} = \frac{R^6_0}{k_{FRET}\tau_D} \quad (16)$$

yields too small values of interchromophoric distances d_{FRET} for the peryleneimide chromophores in the order of 23 Å, despite the expected 28 Å from molecular-modeling structures (Chart 1). The only reason for this discrepancy can be the wrongly estimated value of R_0 because of the too simplified assumption of the dipole−dipole orientation factor κ^2 value of 2/3, which is strictly valid only for a random orientation of the chromophores. Here, this assumption is not true anymore, because of the attachment of chromophores into the dendrimer backbone. The values of κ^2 have been calculated from the three-dimensional molecular mechanics structures by eq 17

$$\kappa = \sin(\delta_D)\sin(\delta_A)\cos(\varphi_{DA}) - 2\cos(\delta_D)\cos(\delta_A) \quad (17)$$

where φ_{DA} is the azimuthal angle between the involved transition dipole moment directions of the energy-donor D and energy-acceptor A, and δ_D and δ_A are the angles between the corresponding dipole directions of D and A with the internuclear D−A axis, respectively. Indeed, average values of around 0.8 are obtained for the chromophore orientations in the meta-substituted dendrimers, confirming that the approximation of $\kappa^2 = 2/3$ made previously[19] was reasonable. However, for the para-substituted dendrimers, the average κ^2 value is clearly larger, being around 2.1. The ratio of the calculated κ^2 values for the para vs the meta series is about 2.6. This value is in nice agreement with the respective ratio of the experimentally determined hopping rate constants, being about k_{hopp}(para)/k_{hopp}(meta) = 2.3 or, if the slightly different interchromophoric distances ($d \cong 26$ Å for meta and $d \cong 28$ Å for para) are taken into account, being about $k_{hopp}d^6$(para)/$k_{hopp}d^6$(meta) = 3.5. Consequently, the faster energy-hopping kinetics in the para series can directly be traced back to a better orientation of the peryleneimide chromophores toward each other, yielding a much larger Förster interaction radius R_0 of 44 Å than in the meta series. Employing this value of R_0 in eq 16 indeed leads to values of $d_{FRET} = 27-28$ Å (Table 2), which agree with the average interchromophoric distances from molecular mechanics modeling.

Intramolecular Excitation Energy Trapping. The terrylene chromophore in **G1R3ter_p** can be expected to act as an energy sink for the energy harvested by the peryleneimide chromophores excited in their absorption maximum at 495 nm. This expectation is derived from the large overlap integral $J = 4.2 \times 10^{15}$ M^{-1} cm^{-1} nm^4 and the correspondingly large interaction radius $R_0 = 60$ Å, calculated by eqs 13 and 14 using the spectral data of **G1R3_p** and a terryleneimide model chromophore ($\epsilon_{max} = 80.000$ M^{-1} cm^{-1},[18] $\phi_f = 98\%$) and assuming $\kappa^2 = 2/3$ as a first approximation for an average of all possible chromophore orientations. Furthermore, by employing a distance d_{FRET} of about 28 Å between the donor and acceptor chromophores, that was also obtained for the peryleneimide interchromophoric distances (Table 2) and that can be expected from the three-dimensional molecular modeling structure of **G1R3ter_p** (Chart 1d), k_{FRET} in eq 16 predicts an efficient rate constant of energy trapping (k_{trap}) from the perylene to the terrylene imide of about 20 ns^{-1} in **G1R3ter_p**. Experimentally, the steady-state fluorescence spectrum of **G1R3ter_p** (Figure 1b) directly proves the trapping of the excitation energy in the peryleneimides by the terrylene chromophore, because the intense fluorescence band of the terrylene emission at 730 nm is observed by excitation at 495 nm, even though terryleneimide itself does not absorb at this wavelength, while, on the other hand, the fluorescence band of the peryleneimide at 560 nm in **G1R3ter_p** is strongly quenched as compared in **G1R3_p** or **G1R4_p**. Quantitative information can be extracted from the drop of the fluorescence quantum yield of the peryleneimide emission in **G1R3ter_p** ($\Phi_f = 4\%$) with respect to that in **G1R3_p** ($\Phi_f = 98\%$).

Using eq 18[29,30]

$$\eta_{trap} = 1 - \frac{\Phi_f^D(AD)}{\Phi_f^D(D)} = 1 - \frac{\tau_f^D(AD)}{\tau_f^D(D)} \quad (18)$$

the energy-trapping efficiency η_{trap} is calculated to be 95%, which, in accordance with the above considerations, yields a quenched mean donor lifetime τ_f^D(AD) of around 160 ps.

The time evolution of the energy-trapping process can visually be followed by the time-resolved emission (TRES) spectra in Figure 3. One can see that in the first 500 ps, the intensity decrease of the peryleneimide band at 560 nm is associated with a concomitant intensity increase or rise of the terryleneimide band at 740 nm, proving the precursor−successor relationship for the donor and acceptor population, respectively. The kinetics for both band maxima are well described by a mean decay and rise time of about 200 ps, which is in good agreement with the value expected from the steady-state considerations using eq 17.

Moreover, the first time-resolved fluorescence spectrum in Figure 3 obtained within the first 80 ps of the arrival of fluorescence photons demonstrates another interesting feature. Already at this early time, terryleneimide emission is observed. This indicates that another but more rapid energy-transfer process from the perylene to the terrylene occurs that is faster than the fwhm (ca. 70 ps) of the detection for this measurement.

The single photon timing global fluorescence decay analysis, which is more precise in determining decay and rise times, indeed reveals that a single rise time is insufficient to fit the experimental decay curves (Figure 2). Instead of only a single decay and rise time, two decay and rise times are recovered, namely, 172 and 52 ps. This means that two channels of energy trapping occur related to two different interaction types or strengths between peryleneimides (donor) and the terryleneimide (acceptor) chromophore.

Very important quantitative information is given by the relative amplitudes of these two time constants in the donor and acceptor emission. The global analysis of decays at several emission wavelengths confirms that the 172 ps component is

Scheme 1. Kinetic Model for Energy Hopping and Trapping Processes in **G1R3Ter_p**

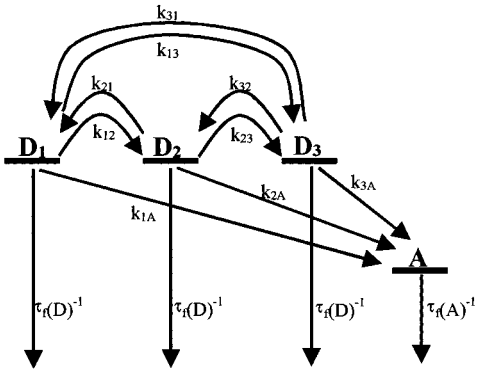

connected with 2/3 of the decay as well as −2/3 of the rise components, while the 52 ps component is associated with the residual 1/3 of the decay as well as −1/3 of the rise components (Table 1). This indicates that on average two peryleneimide chromophores experience a slower energy transfer and a faster energy transfer process.

To simulate the experimental decay behavior, we applied the general kinetic model presented in Scheme 1 and tested different rate constants, k_{ij} for the donor−donor hopping processes and k_{iA} for the donor−acceptor energy trapping processes, among the three donor species and one acceptor species and solved the associated differential equations according to eqs 5−7. Finally, only two basic kinetic models cannot be rejected but can account for the observed time constants and their amplitude ratios as well as for the observed anisotropy decay behavior. Both models involve two fully equivalent peryleneimide chromophores D_1 and D_2 among which energy hopping occurs bidirectionally with k_{ij} $\{i, j = 1, 2\} = k_{hopp} = 4.6$ ns^{-1}, and which energy is trapped by the terrylene acceptor A with a rate constant $k_{1A} = k_{2A} = k_{trap1} \cong 5.5$ ns^{-1}. The fluorescence lifetime of the donors and acceptor is in both models $\tau_f(D) = 4$ ns and $\tau_f(A) = 2.5$ ns, respectively. The nonradiative behavior of the third donor D_3 determines which of the two alternative models is correct. The first model capable of explaining the observed amplitude ratios and decay times considers the single donor chromophore D_3 as either being not involved in the energy hopping (k_{ij} $\{i, j = 3, 3\} = 0$ ns^{-1}), or it only collects the energy from other donors (unidirectional energy transfer); its energy is faster trapped by the terrylene acceptor chromophore with a rate constant of about $k_{3A} = k_{trap2} \cong 20$ ns^{-1}. The second alternative model considers the condition that the third donor chromophore is also fully involved in the donor−donor energy-hopping process, that is, all k_{ij} $\{i, j=1, 2, 3\} = k_{hopp} = 4.6$ ns^{-1}, but that its energy is trapped substantially faster than in the first model, that is, $k_{3A} = k_{trap2} > 20$ ns^{-1}.

Regardless which of the two models is correct, one of the donors experiences at least four times faster energy trapping by the acceptor. The residual question is which physical reasons can explain this phenomenon of dual energy-trapping efficiencies. An intramolecular exciplex formation between donor and acceptor can also be excluded for various reasons, that is, because the donor and acceptor emission spectra are not changed with respect to the model compounds (**G1R1_p** and terylene-imide), an additional decay time for exciplex-type emission is absent, and the molecular modeling results indicate that a close contact between two chromophores is unlikely in the present para series of multichromophoric dendrimer compounds.

The only explanation for the occurrence of a very fast and a slower energy trapping is that on average one of the three donor chromophores takes a much better through-space orientation or smaller interchromophoric distance toward the terrylene acceptor than the other two. To evaluate this possibility, different conformations were modeled,[27] and the chromophore−chromophore center−center distance (d) and orientation (κ^2) were inspected. For example, the rate constants k_{FRET} calculated by eq 13 and 16 using the obtained values of κ^2 and d for the donor−donor energy hopping in **G1R3_p** and **G1R3ter_p** are all very similar and in the range of 2.8−3.6 ns^{-1}. These values, as well as the similarity of all calculated rate constants, are consistent with the experimental value of $k_{hopp} = 4.6$ ns^{-1} and the experimental observation of a single (anisotropy) decay time related to energy hopping and the anisotropy ratios β_2/r_0 pointing to full hopping among all donor chromophores.

On the other hand, a much larger variation of k_{FRET} values calculated on the basis of molecular modeling of **G1R3ter_p** for donor−acceptor chromophore pairs is found—values of k_{FRET} between 0.3 ns^{-1} and mostly 100 ns^{-1}. But in certain cases, where the distances between donor and acceptor come small (16 Å), values up to 1000 ns^{-1} are found. The crucial spatial coordinate seems to be the rotation angle of the bulky and oblate-shaped terryleneimide acceptor. Depending on this angle, this acceptor chromophore can come very close to one *single* donor chromophore, from which the energy trapping might be very fast. Therefore, the experimentally observed rise time values could be a complex combination of rotation, energy hopping, trapping, and fluorescence rate constants.

Conclusions

The dynamics of intramolecular energy hopping and energy trapping in a series of shape-persistent polyphenylene dendrimers substituted in para position at the rim with peryleneimide chromophores and a terryleneimide energy-trapping chromophore are quantitatively studied. Because of the well-defined molecular core structure and high shape persistence, which is responsible for the spatially well-separated energy donor and acceptor chromophores, both energy hopping and trapping can quantitatively be described in terms of Förster-type resonance energy transfer.

The energy hopping takes place among all peryleneimide chromophores with a hopping rate constant experimentally determined to be $k_{hopp} = 4.6$ ns^{-1}. This value agrees with theoretically derived rate constants on the basis of molecular modeling structures. By a comparison with previous photophysical studies on a similar series of polyphenylene dendrimers,[19] where the peryleneimide chromophores were attached in meta instead of para position, the importance of the dipole orientation factor κ^2 could experimentally be demonstrated in excellent agreement with the theoretical Förster equation. While the value of $\kappa^2 = 0.8$ in the meta series yields a hopping rate constant of $k_{hopp} = 2$ ns^{-1}, the improved orientation of peryleneimide chromophores in the para series as connected with a larger κ^2 value of about 2.1 leads to the observed more than two times faster hopping dynamics.

A terryleneimide chromophore attached to the dendrimer rim traps more than 95% of the excitation energy collected by three peryleneimides over a distance of ca. 28 Å. The energy of two of the peryleneimide donor chromophores is trapped with a rate that is similar or only slightly larger than that of the energy hopping, while on average one of the three donor chromophores transfers its energy to the trap chromophore at least four times faster. Molecular modeling based structures tentatively indicate

that the rotation of the terryleneimide acceptor group can lead to a much smaller distance to one *single* donor chromophore, which could explain the experimentally observed amplitude ratios of the rise times and the trapping decay time.

Consequently, the novel molecular design of this type of multichromophoric dendrimers allows investigating experimentally the theory of Coulombic energy transfer.

Acknowledgment. The authors gratefully acknowledge the F.W.O. and DWTC (Belgium) through IUAP-IV-11 and the European Science Foundation through SMARTON for their continuing support. M.M. thanks the EC through TMR-Sisitomas for a postdoctoral fellowship.

JA010570E